

**Morphology and crystallography of electromigration induced transgranular slit failures in aluminum alloy interconnects**

J.E. Sanchez, Jr.\* , V. Randle<sup>+</sup>, O. Kraft, E. Arzt

Max-Planck-Institut für Metallforschung,  
and University of Stuttgart, Stuttgart, Germany

<sup>+</sup>Dept. Materials Engineering, University of Wales, Swansea, Wales, UK

\*present address: Advanced Micro Devices, Sunnyvale, CA 94088

ABSTRACT

Microstructural and crystallographic characterizations of electromigration induced voiding and damage in Al and Al-2% Cu interconnects are presented. Scanning electron and focussed ion beam micrographs show that extended voiding in wide lines and transgranular slit voids in near bamboo lines are the preferred failure morphologies. Electron back scattered diffraction analysis of transgranular slit failure sites show a preferred  $\langle 110 \rangle$  slit void orientation. Estimates of stresses required for stress assisted void growth in unpassivated interconnects are shown to be reasonably close to measured stress levels in films and interconnects. The transgranular void process is shown to be preferred over boundary voiding based on usual estimates for the variation of surface energy and random boundary energies in Al. Finally, line edge void growth into transgranular slit failures at favorably stressed and crystallographically oriented grain sites is presented as an empirical model for the observed electromigration induced failures in near bamboo interconnects lines.

1. INTRODUCTION

There remains a considerable amount of research concerned with electromigration and interconnect reliability driven by the continuing demands for increased performance in advanced integrated circuits. Moreover these requirements will increase as devices continue to reduce in dimension and increase in circuit integration. A major factor influencing the reliability research is the lack of understanding of the basic processes responsible for failure. The forces leading to failure are well known to be mass flux divergences due to electromigration and the large hydrostatic stresses<sup>1</sup> in confined passivated lines. However local mechanistic descriptions of the voiding and hillocking effects induced by these applied forces are not available. Many empirical and microstructural factors are known to affect the average and distribution of failure times of Al-based alloy interconnect structures. For example, increased (111) fiber texture<sup>2</sup>, large and uniform Al grains<sup>2,3</sup>, and certain alloying additions (such as Cu<sup>4</sup>, Ti<sup>5</sup>, Pd<sup>6</sup> and Sc<sup>7</sup>) are known to (often dramatically) increase the lifetimes of interconnects under accelerated electromigration testing conditions. The microstructural factors influencing lifetimes of the hydrostatically stressed passivated interconnects are not as well characterized, however the above factors are expected to generally improve interconnect performance in a similar manner.

Interconnect geometry is also known to affect reliability performance in several ways. The electromigration median time to failure (MTF) and the deviation in time to failure (DTF) increase<sup>3,8</sup> as the line width-grain size ratio (w/d) decreases below  $\sim 1$ . The microstructural and geometrical factors are further confounded since the interconnect microstructure (grain size and second phase distributions) is in part determined by interconnect thickness (h) and width. The positive effect of thicker and narrower

interconnects on electromigration MTF is described as due to the evolution of bamboo grains<sup>9</sup> which span the line width, eliminating boundary paths for rapid diffusion lengthwise along the interconnect. However stress induced failures are observed only for interconnects with  $w < 3 \mu\text{m}$ <sup>10</sup>, that is, as both  $w/h$  and  $w/d$  approach  $\sim 1$ . This effect is described as due to the change of the passivated interconnect stress state from largely biaxial at large  $w/h$  to principally triaxial (hydrostatic)<sup>11</sup> as  $w/h \sim 1$ . A final complication is that the effects of confinement stresses and electromigration may interact<sup>12</sup> to further reduce interconnect performance during accelerated electromigration testing.

Mechanistic descriptions of the processes responsible for interconnect failure should, in addition to providing for the above microstructural and geometrical effects, predict the general shape or morphology of the failure site. Therefore, post-mortem characterizations will be helpful in determining those mechanisms or differentiating between proposed models. It is significant that the morphology of electromigration induced damage and failures is a function of  $w$ <sup>13</sup>. A general trend towards smaller volume voids with decreasing  $w$  persists even when large volume but *non-fatal* voids are present on the same line<sup>13</sup>. This suggests a difference between both the fatal and non-fatal void morphologies, and the processes which create them, which increases with decreasing  $w$ <sup>14</sup>. This trend towards smaller fatal void size is also observed with increasing applied current density<sup>15</sup>. Characterizations of fatal electromigration void sites in near-bamboo Al, Al-Cu, and Al-Cu-Si interconnects have revealed that often open circuits are due to transgranular slit voids<sup>13,14,16,17</sup>, that is, voids that traverse the line width through grains and not along pre-existing boundaries. Such transgranular slit failures (TSF) are observed in unpassivated as well as passivated interconnects, and are also similar to the failure morphologies due to stresses alone in passivated lines<sup>18</sup>. This leads to the hypotheses that such voiding is a general interconnect failure mechanism in bamboo or near-bamboo interconnects, and that stress effects are relevant for electromigration processes in unpassivated lines<sup>16</sup>.

We present further scanning electron and focussed ion beam (SEM and FIB, respectively) microstructural characterizations of electromigration induced damage and failures in unpassivated Al and Al-2% Cu interconnects. The results include the determination of the crystallographic orientations of the TSF and of the grains containing them using electron back scattered diffraction analysis (EBSD)<sup>19</sup>. We discuss preliminary calculations for the stress induced "fracture" of interconnects leading to TSF formation. Finally we present an analysis that suggests that for reasonable estimates of Al surface and boundary energies transgranular voiding is preferable to intergranular voiding along pre-existing boundaries.

## 2. EXPERIMENTAL

Pure Al films (0.5  $\mu\text{m}$  thick) were sputter deposited in a batch system onto 100 mm Si (100) thermally oxidized substrates at room temperature. Deposition rate was  $\sim 0.1 \mu\text{m}/\text{minute}$  with the Ar pressure at  $3 \cdot 10^{-3}$  torr. Base pressure of the system was less than  $4 \cdot 10^{-7}$  torr. Films were then annealed at 400°C for 45 minutes in forming gas and were subsequently 'laser reflowed' using an XMR 7100 system with a XeCl laser operating at 0.308  $\mu\text{m}$ . The wafers were preheated to 400°C prior to the laser reflow treatment. The laser energy dose was  $3.2 \text{ J}/\text{cm}^2$  with a pulse duration of  $\sim 20$  nanoseconds as the laser scanned the wafer. Final grain size in this film was approximately 4  $\mu\text{m}$  as measured by transmission electron microscopy. Electromigration test circuit lithography and dry etching were performed using industry standard techniques to produce arrays of parallel lines 1.0 mm long and ranging from  $\sim 1.0 \mu\text{m}$  to  $\sim 6.0 \mu\text{m}$  in line width. Several other test circuit arrays consisting of Al-2 wt.% Cu interconnects with similar

line widths and geometry were also produced, as described elsewhere<sup>13</sup>. All circuits were unpassivated and tested at wafer level using constant voltage conditions<sup>20</sup> which preserve the failure site<sup>14</sup> at open circuit, allowing for microscopic examination of the damage and failure. Test temperatures were typically between 200°C and 225°C, and current densities were in the range of 1 - 2  $10^6$  A/cm<sup>2</sup>. Quantitative measurements of the fatal void size, void-hillock spacing, and fatal void shape were made from SEM images of the electromigration induced damage and have been presented elsewhere<sup>15</sup>. FIB images taken with an FEI Co. 611 system were used to determine the paths of fatal voids, i.e., along boundaries or through grain interiors. The FIB technique relies on the variation of channeling of the Ga<sup>+</sup> beam in the film to induce bright contrast (scattering of the beam near the surface) or dark contrast (scattering deeper in the film as the beam channels) in order to distinguish grains and grain boundaries<sup>16</sup>. EBSD patterns of specific grains with fatal voids were analyzed to provide the crystallographic orientation of both the fatal void and the grain containing it.

### 3. RESULTS

SEM Fig. 1 illustrates the 'erosion' voiding morphology induced by electromigration in wide ( $\sim 6 \mu\text{m}$ ) Al-2% Cu lines. Note that voids presumably along grain boundaries form a wide network of damage which leads to open circuit. w/d is  $\sim 5$  for these lines so that there are many boundary pathways and sites for damage formation and accumulation. This clustering of void damage is presumably due to preferential sites of mass flux divergence at particular boundary configurations. Such 'active' boundaries may serve as repeating sites for damage as voids migrate away and new voids form. Voiding in wide lines is typically confined to sites within the line and not along the line edge. This damage morphology corresponds closely to those found in many previous observations. However note also in Fig. 1 the regions of bright contrast identified as the Cu rich Al<sub>2</sub>Cu equilibrium  $\Theta$  phase at boundary sites do not

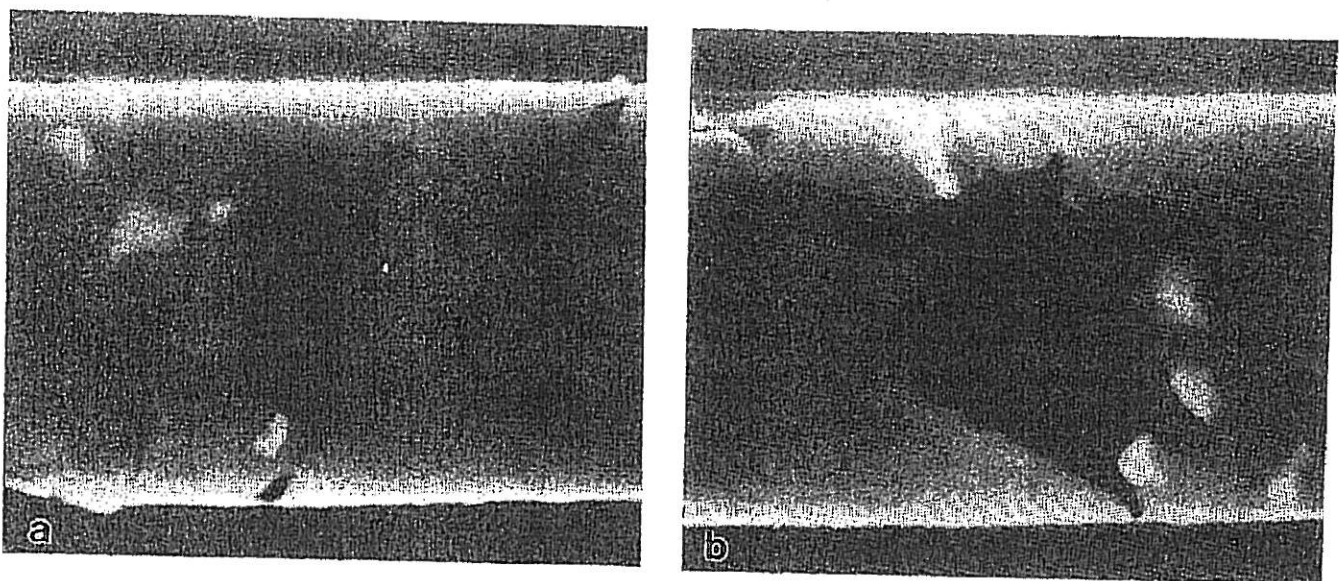


Fig. 1 SEM micrographs of electromigration induced voiding in  $\sim 6.0 \mu\text{m}$  wide interconnects with w/d  $\sim 5$ . a) Shows a network of boundary voiding eventually at sites within the line. b) Shows a large erosion void prior to failure. Note in both micrographs that the presence of the Al<sub>2</sub>Cu  $\Theta$  phase does not prevent voiding.



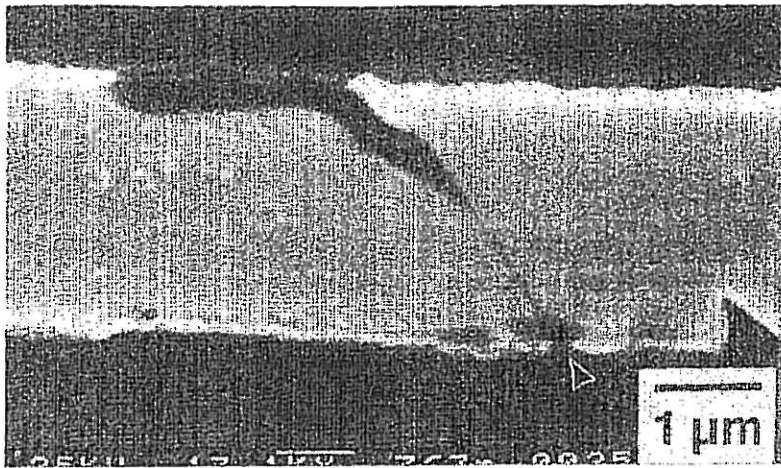


Fig. 2. SEM micrograph of a narrow slit failure in Al-2% Cu interconnect. Line width is  $2.5 \mu\text{m}$  and  $w/d < 2$ . Note that the slit appears to originate or grow from the edge void on the interconnect (at top). Note also the wedge shaped edge void at the bottom-right in the micrograph.

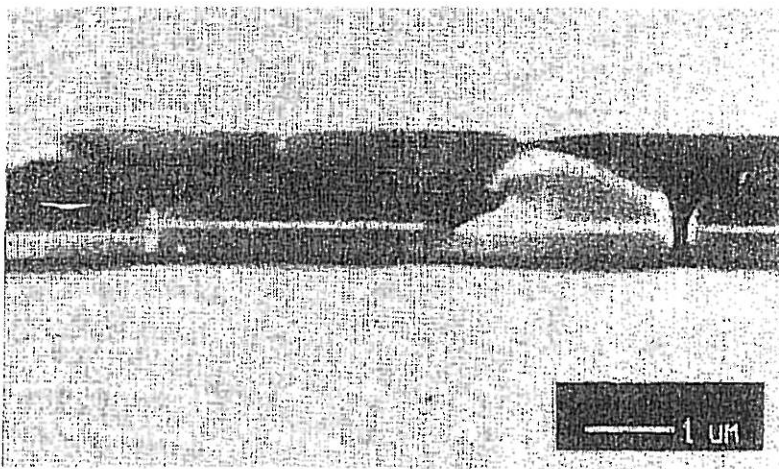


Fig. 3. FIB micrograph of laser reflowed Al interconnect showing extensive but non-fatal electromigration voiding at triple points connecting boundaries parallel to the applied field. A corresponding hillock is off the field of view to the left in the direction of mass and electron flow. Line width is  $1.8 \mu\text{m}$ .

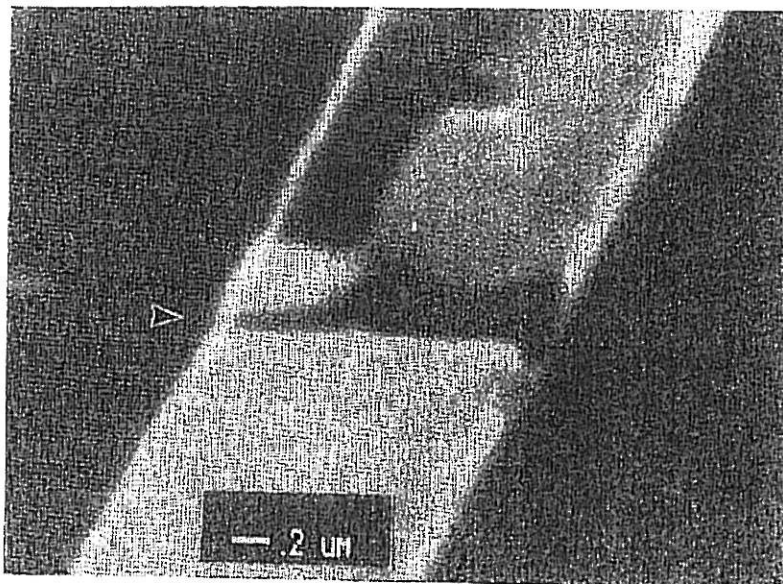


Fig. 4. FIB micrograph of a laser reflowed Al electromigration induced transgranular slit failure in a laser reflowed Al interconnect. It is evident that the void originated at the boundary/edge site on the right, but continued growth (to the left) across the grain in bright contrast (arrow). Line width is  $1.8 \mu\text{m}$ .

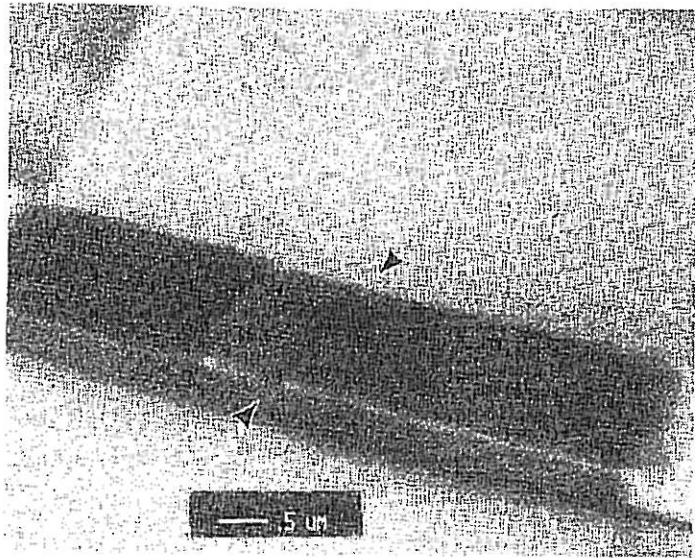


Fig. 5 FIB micrograph of a transgranular slit failure (arrows) in laser reflowed Al interconnect. Line width is  $1.8 \mu\text{m}$ . The grains in bright and dark contrast reveals that the slit failure is not located at a boundary.

prevent voiding in their nearby region. This is in contrast to the model for the beneficial effect of Cu in Al alloy interconnects which proposes that mass flux divergence and damage will occur at sites where local sources of Cu, such as  $\Theta$  phases, are depleted<sup>4</sup> from boundary regions.

A sharp slit failure in a narrow Al-2% Cu line is shown in Fig. 2. Here  $w$  is  $\sim 2.5 \mu\text{m}$  and  $w/d < 2$ . Note that the slit void appears to originate from an elongated void along the line edge, where other voids are seen. Edge voiding rather than internal voiding is simply due to the lack of boundary paths and sites for flux divergence within the line as its structure evolves towards bamboo grains. However these voids are evidence that surface or interface diffusion along the line edge leads to flux divergence. Void motion along the line edge is further evidence of significant mass flux there. It is also possible that voids may form where boundaries meet the line edge. However the growth of 'edge' voids along the line, as shown in Fig. 2 and in Fig. 5 of reference 5, reveal the flux activity there by surface or interface (along the native Al oxide/Al interface) processes.

Often large non-fatal voids may be seen in narrow lines which failed elsewhere<sup>13</sup> by the slit morphology. Fig. 3 shows an FIB image of the extensive but non-fatal local voiding in a  $1.8 \mu\text{m}$  wide laser reflowed Al interconnect. The open circuit failure in this line occurred elsewhere by the slit void process. These large voids may cause local current density increases of 5-10 times, much larger than the current crowding due to shallow edge voids prior to failure. This suggests that decreased reliability in narrow interconnects is primarily due to the slit failure mechanism<sup>14,16,17</sup>.

Fig. 4 shows an FIB image of a transgranular slit failure (TSF) which appears as part of a void situated at a boundary (on the right edge of the line). The narrow portion of the void (on the left) crosses the grain as confirmed by EBSD analysis (below). Fig. 5 illustrates another TSF clearly apart from any boundary. Further FIB observation of these voids in several tilt and rotation orientations confirmed the TSF nature.

The results of EBSD analysis of three typical TSF showed a growth direction less than  $10^\circ$  from  $[110]$ , (i.e.,  $\sim 10^\circ$ ,  $\sim 5^\circ$ , and exactly  $[110]$ ). The fiber orientations of these three grains was  $29^\circ$ ,  $7^\circ$ , and  $3^\circ$  from  $\langle 111 \rangle$ , respectively. However this is hardly indicative of a preference for TSF in  $\langle 111 \rangle$  fiber oriented grains since such texture is typical for most films.

#### 4. DISCUSSION

The TSF observed the Al and Al-2% Cu interconnects are similar to those found in studies<sup>13,14,16</sup> of unpassivated Al, Al-2% Cu, and Al-2% Cu-1% Si lines and passivated Al-2% Cu lines<sup>17</sup>. In one recent study<sup>17</sup> of passivated interconnects the TSF morphology was almost exclusively responsible for failure. This suggests that the effect of passivation is to increase the proportion of failures due to TSF. Since extensive voiding requires a corresponding material accumulation at the surface, the effect of passivation may be to prevent surface hillocking and extrusions thereby limiting large volume erosion voiding, leaving TSF as the more likely and common failure mechanism. Further comparisons between unpassivated and passivated interconnect failure sites are required to test this hypothesis.

##### 4.1 Crystallography of transgranular slit failures

The EBSD results are somewhat in agreement with selected area diffraction results obtained by transmission electron microscopy<sup>17</sup>. In that study the TSF were closely aligned along  $\langle 110 \rangle$  directions with faces parallel to (111) plane, and it was proposed that  $[110]$  is the TSF growth direction. The more limited data here are somewhat consistent with the alignment of the TSF with  $\langle 110 \rangle$ , but the orientation of faces with (111) was not confirmed, in part due to the poor characterization of the spatial orientation of the TSF through the line thickness. Further analysis is required in order to more precisely index the TSF faces in this study.

##### 4.2 Stress assisted slit voiding

Since the TSF morphology is similar to stress induced failures, it is interesting to consider slit void formation due to or assisted by stresses. Two essential features of the fatal void morphology should be addressed: 1) the magnitude of stresses required to propagate a void through the interconnects, and 2) the preference for the transgranular pathway rather than along pre-existing boundaries, to be discussed in the next section.

Unpassivated lines with aspect ratio  $w/h$  of  $\sim 2$  or less are expected to sustain only uniaxial stresses, since the only line constraint is along the length direction. Lateral (defined as in the width direction) relative thermal strain imposed by the substrate will be relaxed through most of the line thickness since the line is free to expand or contract in the width direction. Direct measurement of the stresses by x-ray techniques<sup>21</sup> in similar unpassivated lines during thermal treatments confirms this stress state. Preliminary calculations<sup>22</sup> estimate that a stress of  $\sim 200$  MPa will be required to "fracture" an interconnect of the type illustrated here. The sources for this stress may be thermal mismatch between the Al and the Si substrate, and mass flux divergence due to electromigration along boundaries in non-bamboo segments of the line. While the magnitude of the stress required is greater than those measured<sup>21</sup>, it is not unreasonably high. Clearly, however, possible stress increases due to the sources described above require that stress relaxation and yielding processes do not limit stress build-up. Note that in this discussion we considered

only uniaxial stresses, while the stresses induced by the confinement of passivation are triaxial. Further work is required to determine the proper application of the fracture mechanics relevant for interconnect voiding and failure processes.

#### 4.3 Surface energetic analysis of transgranular voiding

The preference for TSF rather than intergranular voiding may be analyzed from a surface energetic perspective<sup>23</sup>. For example, consider 'crack' propagation along a boundary with specific energy  $\gamma_b$ . Crack opening along the boundary creates new surfaces of specific energy  $\gamma_{sb}$ . The net (specific) energy required for failure in this case is

$$E_b = 2 \gamma_{sb} - \gamma_b \quad (1).$$

That is, the boundary reduces the energy required for crack opening there by an amount  $\gamma_b$ . Alternately, consider that the energy required for intragranular crack opening is given by

$$E_s = 2 \gamma_s \quad (2),$$

where  $\gamma_s$  is the specific energy for surfaces created by this 'cleavage' process. As can be seen from Fig. 4, often the TSF process is preferred even at sites where void opening may progress along adjacent boundaries. This preference can be expressed energetically as  $E_b > E_s$ , or

$$(2\gamma_{sb} - \gamma_b) / 2 \gamma_s > 1 \quad (3).$$

However, given that typical boundaries will be random with high misorientation, the surfaces created by intergranular voiding will in general be of random orientation and of high (maximum) surface energy  $\gamma_{sb}$ . Conversely, intragranular void propagation is not constrained to follow boundaries and may select and proceed along low index-low surface energy planes, such that  $\gamma_s$  is generally low (minimum). This fatal void plane orientation has been confirmed by transmission electron diffraction analysis<sup>17</sup>. Typical differences between  $(\gamma_s)_{\max}$  and  $(\gamma_s)_{\min}$  for FCC metals are approximately 20%, yielding  $\gamma_{sb} - \gamma_s \sim 1.2$ . The inequality (3) may then be restated as

$$1.2 - (\gamma_b / 2\gamma_s) > 1 \quad (4),$$

$$\gamma_b / \gamma_s < 0.4 \quad (5),$$

for preferred intragranular void opening. A usual estimate<sup>24</sup> for  $\gamma_b/\gamma_s$  is  $\sim 1/3$ . Therefore under these assumptions it is reasonable to conclude that intragranular void propagation leading to TSF is a likely process for failure.

While it has been proposed<sup>25</sup> that increased interconnect strength may improve electromigration lifetime, no experimental evidence exists to prove such a relationship. Methods for film strengthening by



microstructural control can be proposed given an understanding of plastic flow in continuous films. Yet it is not certain that increased film strength translates into improved properties in uniaxially stressed (narrow, unpassivated) lines or in passivated lines subject to large hydrostatic stresses. Further work is required in order to determine the role of interconnect microstructure on the transgranular slit failure mechanism and on damage processes in general.

#### 4.4 Mechanism for transgranular slit failures

It is worthwhile to discuss the role of surface or interface diffusion along line edges in voiding and failure processes in near bamboo lines. As described above, the lack of significant voiding within line interiors is due to the reduction of triple points and boundary segments parallel to the applied field. Voiding and void motion along the line edge show that flux activity there is an effective alternative to boundary pathways. Evidence for such flux has existed for some time. d'Heurle<sup>26</sup> observed large voids and hillocks in pad areas of Al single crystal lines subjected to accelerated electromigration testing. Pierce<sup>27</sup> similarly found extensive voids and hillocks in pads connected to bamboo grained Al lines. More recently, Hasunuma<sup>18</sup> and Shingubara<sup>28</sup> found electromigration induced voids in passivated Al single crystal lines. Longworth<sup>29</sup> recently concluded that interfacial diffusion was responsible for much of the electromigration induced damage in bicrystal Al lines.

Often transgranular slit electromigration failures appear to emanate from line edge voids. These wedge shaped voids and fatal slits are also found in passivated lines subjected to high hydrostatic stresses. It is possible therefore that these edge voids serve as nuclei for the fatal slit voids. In this model flux divergences along the line edge produce wedge voids, which often migrate along the line<sup>13</sup>. The failure process may occur as these voids reach a bamboo grain oriented under conditions favorable to slit void growth. These conditions are; 1) void location at a region of net tensile stress, for example at the 'upstream' end of a line segment containing boundaries and triple points parallel to the direction of electromigration; 2) grain crystallographic orientation such that a preferred void growth [110] direction and (111) plane are each nearly perpendicular to the line, so that void growth efficiently relieves the uniaxial stresses (in the unpassivated lines). These conditions are typically satisfied for many TSF observed in this and other studies. Further work will help clarify the role of microstructural, texture, and stress effects and the effects of passivation on the transgranular slit voiding process.

### 5. CONCLUSIONS

The morphology of electromigration damage and open circuit failures were shown to be functions of line width. Internal voiding leads to extended damage networks in wide (large w/d) lines whereas line edge voids lead to small volume slit voids in narrow interconnects. The crystallographic orientation of several transgranular slit failures and associated grains was determined by electron back scattered diffraction analysis. Slit failure growth direction was  $\sim \langle 110 \rangle$ , consistent with results determined by transmission electron diffraction analysis. Failed grain orientations varied by up to  $\sim 30^\circ$  from ideal (111) texture, again consistent with other results. Preliminary estimates for stresses required for interconnect cracking were shown to be reasonably close to measured stress levels in thin films and interconnects. An energetic analysis based on usual estimates for variations in Al surface and boundary energies shows that transgranular void or crack growth may be preferred to void growth along boundaries. The growth of line edge voids into transgranular slit failures at grain sites with the favorable [110] growth direction and under sufficient tensile stresses was presented as a mechanism for the observed failures.



## 6.0 ACKNOWLEDGMENTS

We appreciate the assistance of both Dr. Richard Young (FEI Co., Cambridge, UK) with FIB microscopy and Dr. Stefan Bader (Stanford University, and Max-Planck-Institut) with interconnect sample preparation. One author (JES) would like to acknowledge the support of the Max-Planck Society and the express appreciation for the hospitality and productive support during his tenure at the Max-Planck-Institut in Stuttgart, Germany.

## 7. REFERENCES

1. B. Greenebaum, A.I. Sauter, P.A. Flinn, W.D. Nix, "Stress in Metal Lines Under Passivation; Comparison of Experiment With Finite Element Calculations," *Applied Physics Letters*, Vol. 58 (17), pp. 1845-1847, 1991.
2. S. Vaidya, A.K. Sinha, "Effect of Texture and Grain Structure on Electromigration in Al-0.5% Cu Thin Films," *Thin Solid Films*, Vol. 75, pp. 253-259, 1981.
3. J. Cho, C.V. Thompson, "Grain Size Dependence of Electromigration Induced Failures in Narrow Interconnects," *Applied Physics Letters*, Vol. 54 (25), pp. 2577-2579, 1989.
4. F.M. d'Heurle, "Effect Of Cu Additions on Electromigration in Al Thin Films," *Metallurgical Transactions*, Vol. 2, pp. 683-689, 1971.
5. F. Fischer, F. Nepl, "Sputtered Ti-Doped Al-Si For Enhanced Interconnect Reliability," *Proc. 22nd IEEE International Reliability Physics Symposium*, pp. 190-192, IEEE, Las Vegas, 1984.
6. Y. Koubuchi, J. Onuki, M. Suwa, S. Fukada, "Stress Migration Resistance of Al-Si-Pd Alloy Interconnects," *Proc. 6th VLSI Multilevel Interconnection Conference*, vol. TH-0259-2/89/0000-0419, pp. 419-425, IEEE, Santa Clara, 1989.
7. S.-I. Ogawa, H. Nishimura, "A Novel Al-Sc (Scandium) Alloy For Future LSI Interconnection," *Proc. IEEE International Conference on Electron Devices and Materials*, vol. IEEE-IEDM 1991, pp. 10.4.1-10.4.4, IEEE, Washington, DC, 1991 .
8. S. Vaidya, T.T. Sheng, A.K. Sinha, "Linewidth Dependence of Electromigration in Evaporated Al-0.5% Cu," *Applied Physics Letters*, Vol. 36 (6), pp. 464-466, 1980.
9. D.T. Walton, H.J. Frost, C.V. Thompson, "Development of Near-Bamboo and Bamboo Microstructures in Thin-Film Strips," *Applied Physics Letters*, Vol. 61(1), pp. 40-42, 1992.
10. J.T. Yue, W.P. Funsten, R.Y. Taylor, "Stress Induced Voids In Aluminum Interconnects During IC Processing", *Proc. 23rd IEEE International Reliability Physics Symposium*, pp. 126-137, IEEE, Orlando, 1985.
11. A.I. Sauter, W.D. Nix, "Finite Element Calculations of Thermal Stresses in Passivated and Unpassivated Lines Bonded to Substrates," *Thin Films: Stresses and Mechanical Properties II*, M. Doerner, W. Oliver, G. Pharr, F.R. Brotzen Editors, Vol. 188, pp. 15-20, Materials Research Society, San Francisco, 1990.
12. P. Borgesen, "Stress-Induced Voiding and Electromigration," C.-Y. Li, P. Totta, P. Ho Editors, *Proc. First International Workshop on Stress Induced Phenomena in Metallizations*, pp. 219-235, Academic Press, Ithaca, NY, 1991.
13. J.E. Sanchez, Jr., L.T. McKnelly, J.W. Morris, Jr., "Morphology of Electromigration-Induced Damage and Failure in Al Alloy Thin Film Conductors," *Journal of Electronic Materials*, Vol. 19, pp. 1213-1220, 1990.

14. J.E. Sanchez, Jr., L.T. McKnelly, J.W. Morris, Jr., "Slit Morphology of Electromigration-Induced Open Circuit Failures in Fine Line Conductors," *Journal of Applied Physics*, Vol. 72 (7), pp. 3201-3203, 1992.
15. O. Kraft, J.E. Sanchez, Jr., E. Arzt, "Quantitative Analysis of Electromigration-Induced Damage in Al-Based Interconnects," *Materials Reliability Issues in Microelectronics II*, J.R. Lloyd, C.V. Thompson Editors, Vol. 265, pp. 119-124, Materials Research Society, San Francisco, 1992.
16. J.E. Sanchez, Jr., O. Kraft, E. Arzt, "Electromigration Induced Transgranular Slit Failures in Near Bamboo Al and Al-2% Cu Thin Film Interconnects," to appear in *Applied Physics Letters*, Vol. 61 (26), December 1992.
17. J.H. Rose, "Fatal Electromigration Voids in Narrow Aluminum-Copper Interconnect," *Applied Physics Letters*, Vol. 61 (18), pp. 2170-2172, 1992.
18. M. Hasunuma, H. Kaneko, A. Sawabe, T. Kawanoue, Y. Kohanawa, S. Komatsu, M. Miyauchi, "Single Crystal Aluminum Lines With Excellent Endurance Against Stress Induced Failure," *Proc. IEEE International Conference on Electron Devices and Materials*, Vol. IEEE-IEDM 1989, pp. 677-680, IEEE, Washington, DC, 1989.
19. V. Randle, "Experimental Aspects of the Electron Back-Scatter Diffraction Technique for Grain Boundary Characterization," *Materials Science Forum*, Vol. 94-96, pp. 233-243, 1992.
20. C.V. Thompson, J. Cho, "A New Electromigration Testing Technique for Rapid Statistical Evaluation of Interconnect Technology," *IEEE Electron Device Letters*, Vol. 7 (12), pp. 667-668, 1986.
21. P.R. Besser, R. Venkatraman, S. Brennan, J.C. Bravman, "Calculation of Stress Gradients in Thin Al-0.5% Cu/Ti Lines From Strain Gradients Measured as a Function of Temperature Using Grazing Incidence X-Ray Scattering," *Thin Films: Stresses and Mechanical Properties III*, E. Arzt, J. Bravman, W.D. Nix, B. Freund Editors, Vol. 239, pp. 233-238, Materials Research Society, Boston, 1991.
22. J.E. Sanchez, Jr., D. Srolovitz, unpublished research.
23. A.H. Cottrell, "Strengths of Grain Boundaries in Pure Metals," communicated by A.L. Greer, Cambridge University, UK
24. W.W. Mullins, "The Effect of Thermal Grooving on Grain Boundary Motion," *Acta Metallurgica*, Vol. 6, pp. 414-427, 1958.
25. E. Arzt, W.D. Nix, "A Model For the Effect of Line Width and Mechanical Strength on Electromigration Failure of Interconnects with 'Near-Bamboo' Grain Structures," *Journal of Materials Research*, Vol. 6, pp. 731-736, 1991.
26. F.M. d'heurle, personal communication.
27. J.M. Pierce, M.E. Thomas, "Electromigration in Aluminum Conductors Which Are Chains of Single Crystals," *Applied Physics Letters*, Vol. 39 (2), pp. 165-168, 1981.
28. S. Shingubara, Y. Nakasaki, H. Kaneko, "Electromigration in a Single Crystalline Submicron Width Aluminum Interconnection," *Applied Physics Letters*, Vol. 58 (1), pp. 42-44, 1991.
29. H.P. Longworth, C.V. Thompson, "An Experimental Study of Electromigration in Bicrystal Al Lines," *Applied Physics Letters*, Vol. 60 (18), pp. 2219-2221, 1991.